JCTC Journal of Chemical Theory and Computation

QM/MM Studies on the β-Galactosidase Catalytic Mechanism: Hydrolysis and Transglycosylation Reactions

Natércia F. Brás, Pedro A. Fernandes, and Maria J. Ramos*

REQUIMTE, Departamento de Química, Faculdade de Ciências, Universidade do Porto, Rua do Campo Alegre, 687, 4169-007 Porto, Portugal

Received October 6, 2009

Abstract: Carbohydrates perform a wide range of crucial functions in biological systems and are of great interest for the food and pharmaceutical industries. β-Galactosidase from *Escherichia coli* catalyzes both the hydrolytic breaking of the very stable glycosidic bond of lactose and a series of transglycosylation reactions. These reactions are crucial for the development of new carbohydrate molecules, as well as the optimization of their syntheses. In this work we have used computational methods to study the catalytic mechanism of hydrolysis and a set of distinct transglycosylation reactions of a retaining galactosidase, with atomic detail, with lactose as the natural substrate. The ONIOM method (BB1K:AMBER//B3LYP:AMBER calculations) was employed to address such a large enzymatic system. Such a methodology can efficiently account for the stereochemistry of the reactive residues, as well as the long-range enzyme−substrate interactions. The possible importance of the magnesium ion in the catalytic reaction was investigated, and it was found that, indeed, the magnesium ion catalyzes the transformation, lowering the activation barrier by 14.9 kcal/mol. The calculations indicate that the formation of β(1−3) glycosidic linkages is thermodynamically very unfavorable. In contrast, the formation of β(1−6) glycosidic bonds is the most favored, in complete agreement with the enantioselectivity observed experimentally. The data also clearly show the importance of the enzyme scaffold beyond the first-shell amino acids in the stabilization of the transition states. It is fundamental to include the enzyme explicitly in computational studies.

1. Introduction

Oligosaccharides play a large number of crucial functions in biological systems and have attracted the attention of the pharmaceutical industry due to their potential application as therapeutics.[1,2] *Escherichia coli* (*lacZ*) β-galactosidase (EC 3.2.1.23) catalyzes the hydrolysis and transglycosylation of β-D-galactosides.[3,4] Both the amino acid and nucleotide sequences have been determined. The enzyme is a homotetramer, each monomer weighing 116353 Da and having 1023 amino-acid residues displayed in five sequential domains, with an extended segment at the amino terminus. The monomers work independently. The three-dimensional structure of β-galactosidase shows that the active site is located in a deep pocket within a distorted "TIM" barrel. Divalent and monovalent cations are required for full catalytic efficiency. The Mg^{2+} or Mn^{2+} cations provide 5−100-fold activation depending on the substrate used, whereas the Na^{+} or K^{+} cations provide only 0.3−6-fold activation depending on the ion and substrate involved. The active site has two subsites: the first binding site is highly specific for the galactose moiety, whereas the second binding site lacks specificity.[4−6] This ambiguous specificity allows the binding of a wide variety of β-D-galactosides beyond the natural substrate lactose (Figure SI-1 in the Supporting Information). An example is X-Gal (5-bromo-4-chloro-3-indoyl-β-D-galactopyranoside), which is a substrate that incorporates a chromophore. With this substrate, the activity of the enzyme is easily recognized by a distinct change in color. The

* Corresponding author e-mail: mjramos@fc.up.pt.

10.1021/ct900530f
Published on Web 01/13/2010

Scheme 1. General Scheme for the Catalytic Mechanism of β-Galactosidase and a Lactose Molecule

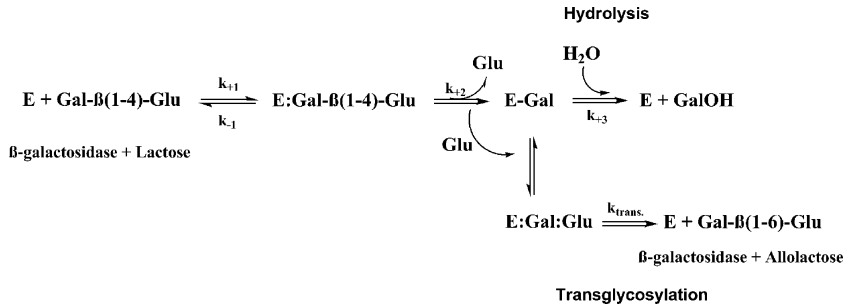

capacity of the β-galactosidase to cleave chromogenic substrates has clearly contributed to its usefulness as a tool of research in molecular biology.[3,6]

Glycosidic linkages are enzymatically hydrolyzed by one of the two major groups of glycosidases: retaining and inverting glycoside hydrolases.[7] β-Galactosidase from *E. coli* is a retaining glycosidase. Thus, it maintains the initial conformation on the anomeric carbon. The proposed catalytic mechanism of this enzyme is believed to occur through a double-displacement reaction involving galactosylation and degalactosylation steps, with the reaction probably proceeding through a covalent galactosyl−enzyme intermediate.[8,9] The active site contains two carboxylic acid residues, which have been identified as Glu461 (proton-donor residue) and Glu537 (catalytic nucleophile group).[6] These two amino acids are approximately 5.5 Å apart. It is well-known that more basic groups, such as glucose, require acid/base catalytic assistance for departure of the leaving group.[7] A magnesium ion is also found close to the active site, although the exact role of this ion in catalysis has always remained unclear.[6,10,11] Kinetic data support the possibility of Lewis catalysis promoted by the Mg^{2+} ion, the possibility of Brönsted catalysis through protonation by the Glu461 residue, or eventually both. Crystallographic studies suggest that the latter hypothesis is the most probable to occur.[6] Simultaneously, Glu537 acts as a nucleophile, forming a covalent galactosyl−enzyme intermediate.

Experimental and computational works suggest that a hydrogen bond between the C_2 hydroxyl group and this nucleophilic residue, already present in the reactants, is shortened at the transition state and further catalyzes the reaction.[7,12] It has also been suggested on the basis of experimental observations and computational work that the enzyme has another strategy for stabilizing the transition state, which corresponds to substrate distortion from a chair to a half-chair conformation, promoted by substrate binding.[7,12] This first step is characterized by the departure of the glucose group. The second mechanistic step of the reaction is supposed to involve the attack of the covalent carbohydrate−enzyme intermediate by a water molecule (hydrolysis) or a sugar molecule (transglycosylation), concomitantly with or followed by the transfer of a proton from a water/sugar to the proton donor, in a reverse mode of the first step (Scheme 1). Some researchers consider that both transition states (TSs) have a mainly dissociative character.[7] The experimental measurements of α secondary deuterium kinetic isotope effects (αDKIEs) suggest that both transition states have substantial oxocarbenium ion character.[13,14] Furthermore, these studies suggest that the reaction rate of the degalactosylation step depends on the acceptor concentration, which indicates that this transition state somehow involves the acceptor molecule and, consequently, is not a pure S_N1 TS, as has been proposed for many other glycosidases.[6]

A large number of oligosaccharides can be synthesized by transglycosylation reactions, even though the yields obtained are typically low (5−20%), as the products are also substrates for the enzyme and undergo hydrolysis. These reactions are supposed to be kinetically controlled, with the yields of the synthesized oligosaccharides depending on the relative rates of the transglycosylation and hydrolysis reactions.[15] The stereoselectivity of the glycosidic bond is a difficulty associated with oligosaccharides synthesis. Experimental data suggest that the transglycosylation reaction catalyzed by β-galactosidase produces preferably allolactose [β-galactopyranosyl-(1−6)-α-glucopyranose] with a yield of ~97%.[3,4,6] This is physiologically important to *E. coli*, as this molecule is the natural inducer for the *lac* operon, which is responsible for the β-galactosidase expression. In that case, it might be expected that, in the transglycosylation enrichment on β-(1−6), the new linkage would be created by a rotation of the glucose molecule immediately after the cleavage followed by the chemical reaction, without it ever leaving the binding pocket.

Other disaccharides can be formed at low levels, particularly when glucose is added to the reaction. Lactose and allolactose are hydrolyzed with equal efficiency (k_{cat} = 60 s^{-1} and K_m = 1 mM for both molecules), whereas only allolactose is produced from the transglycosylation reaction. Furthermore, the values of k_{cat} for allolactose production and hydrolysis are similar, but this balance can be altered by the pH and by the absence of magnesium ions.[6,16]

Mutagenesis studies performed with β-galactosidase show that Glu461, Glu537, Tyr503, Asn460, His357, His391, and His540 residues interact with specific hydroxyl groups of the substrate.[17−20] Juers et al. cocrystallized series of ligands bound to the active site of β-galactosidase, and in the X-ray structures, it was possible to confirm that all of the residues previously identified as catalytically important were indeed positioned in or near the active site.[6] These crystallographic structures show that there are two distinct manners for the binding of ligands, namely, "shallow" and "deep" modes. Phe601 and Trp999 are also considered to be important for the catalytic mechanism. The substrate initially binds in a shallow mode, characterized by stacking on Trp999, estab-

lishing interactions between the side chain of the tryptophan and the ring of the glucose group. Subsequently, the substrate moves into a deep mode, further into the active site. To allow this transition, the side chain of Phe601 rotates, and the 794−804 loop also rearranges.[6] In this conformation, after the first step, the access to the galactosyl−enzyme intermediate by other molecules becomes more restricted.

Our goal with this article is to present a set of calculations that completely elucidate and clarify with atomic-level detail the chemical events involved in the catalytic mechanism of *E. coli* β-galactosidase using lactose as the natural substrate. For that purpose, we have used a large enzyme model and employed the ONIOM method to deal with such a large system, namely, the BB1K:AMBER//B3LYP:AMBER methodology. This enzymatic model can efficiently account for the restrained mobility of the reactive residues, as well as the long-range enzyme−substrate interactions.

2. Theoretical Calculations

X-ray crystallographic structures of the enzyme β-galactosidase complexed with substrate analogues show that the substrate has to bind in a shallow mode. Subsequently, the substrate must move to the deep mode, that is, further into the active site, for catalysis to occur. The 1DP0 protein databank structure of β-galactosidase (at 1.7-Å resolution) was used as the starting point for all computational studies.[6] All water molecules were deleted, with the exception of some conserved waters near the active site that coordinate the magnesium and sodium ions. Hydrogen atoms were added using Insight II software,[21] with all residues in their physiological protonation state. The only exception was the proton-donor residue (Glu461), which was protonated. The geometry optimization of the protein was done in three stages to release the bad contacts in the crystallographic structure. In the first stage, only the hydrogen atoms were minimized; in the second stage, the backbone was minimized; and in the third and final stage, the entire system was minimized. About 1500 steps were used for each stage, with the first 500 steps performed using the steepest-descent algorithm and the remaining steps carried out using conjugate gradient.

A lactose molecule was initially docked into the structure of the optimized unligated β-galactosidase, mimicking the deep mode of binding. To do this, we used GOLD docking software[22] and ChemScore as the scoring function.[23] The program is based on a genetic algorithm that is used to place different ligand conformations in the protein binding site, recognized by a fitting-points strategy.

It is well-known that the hydrogen bridge established between the nucleophile and the 2′-OH group of the substrate is essential for the stabilization of the transition states structures. Therefore, this interaction is conserved among retaining glycoside hydrolases.[12,24] To constrain the docking solutions toward this particular pose, this bridge was maintained through a distance constraint (2.00−2.50 Å) between the two atoms involved. Furthermore, in many glycosidases, the presence of several aromatic residues (Trp, Phe, or Tyr) close to the active site provides the hydrophobic platform common to carbohydrate−protein interactions. Trp568 plays a similar role and displays a position and orientation that promote the packing of the galactose moiety in the deep binding mode. To obtain the correct position for binding, a distance constraint (3.40−3.70 Å) was also included between this aromatic residue and the galactose moiety of the docked lactose. Furthermore, in the docking method, we have taken into consideration whether the acid/base was close and directly positioned for the attack on the glycosidic oxygen. After analysis of all of the solutions obtained, the best docking solution was chosen as the starting structure for the subsequent molecular dynamics study to release the bad contacts in the structure. In the end, we used the final structure to design a large enzymatic model. All molecular dynamics simulations were performed with the parametrization adopted in Amber 8,[25] using the Amber 1999 force field (parm99) for proteins and the Glycam 2004 force field (Glycam-04 parameters) for carbohydrates.[26–28] In this simulation, an explicit solvent model with pre-equilibrated TIP3P water molecules was used, filling a truncated octahedral box with a minimum 12-Å distance between the box faces and any atom of the protein.[29] The complex structure was minimized in two stages. In the first stage, the protein was kept fixed, and only the positions of the water molecules and counterions were minimized. In the second stage, the full system was minimized. Subsequently, using the Langevin temperature equilibration scheme, a 20-ps molecular dynamics (MD) simulation at constant volume and with periodic boundary conditions was run starting from the optimized structures.[30,31] After this, 1 ns of MD simulation was performed. Langevin dynamics was used (collision frequency of 1.0 ps^{-1}) to control the temperature.[30,31] The simulation was carried out using the sander module, implemented in the Amber8 simulations package, with the Cornell force field.[32] Bond lengths involving hydrogens were constrained using the SHAKE algorithm,[33] and the equations of motion were integrated with a 2-fs time step using the Verlet leapfrog algorithm.

The QM/MM calculations performed to determine the enzyme−substrate potential energy surface (PES) were executed using Gaussian 03 software.[34] To perform the study, we used the final structure of the MD simulation, from which we cut a model including a 15-Å radius around the lactose molecule. The system was composed of a total of 2707 atoms. To explore the PES of the catalytic reaction, our system was divided into two layers, within the ONIOM formalism[35,36] as implemented in Gaussian 03. In geometry optimizations, the higher-level layer included almost the entire substrate and the side chains of Glu461 and Glu537 for a total of 49 atoms, and it was treated with density functional theory (DFT) at the unrestricted B3LYP/6-31G(d) level.[37–39] The rest of the system was treated at the molecular mechanics level with the parm99 and Glycam04 force fields. We further froze the positions of the atoms in the outer 5-Å shell of the entire system (Figure 1). For each reaction step, we performed a linear transit scan along the reaction coordinate with a step value of 0.05 Å to locate the geometry of the transition state. In the literature, this procedure is common for large models with QM/MM calculations.[40–42] All linear transit schemes obtained here were smooth and are included in the Supporting Information (Schemes SI-

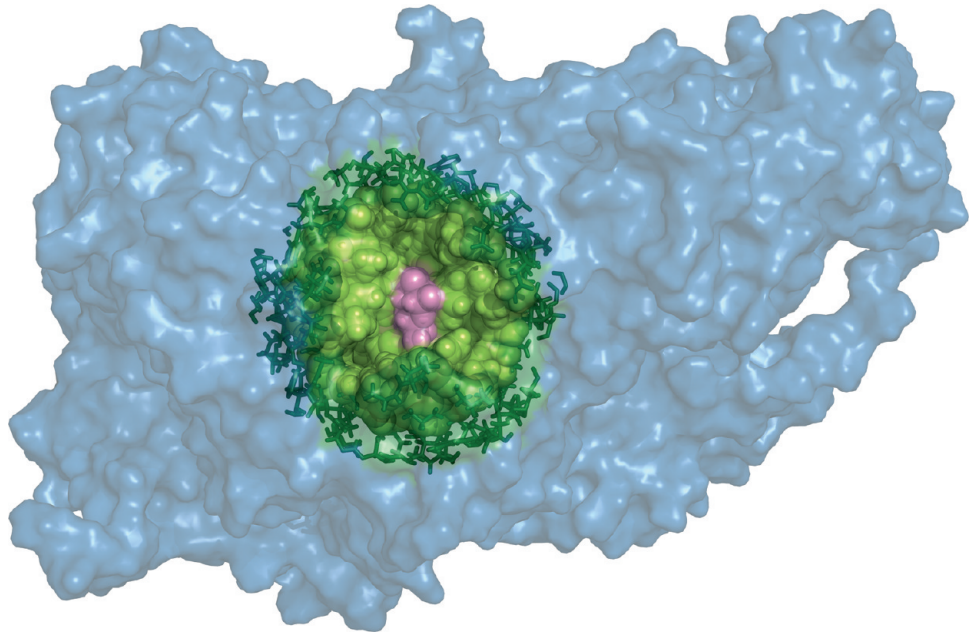

Figure 1. Representation of the enzymatic model studied, which includes a 15-Å radius of the amino acids around lactose. The model system is shown in green. The frozen region (the outer 5-Å shell of the entire system) is represented as dark green sticks. The substrate is colored pink.

1−SI-5). As the interaction between the layers was described at the MM level, we had to recalculate the atomic point charges for all of the atoms involved in bond breaking/bond formation during the scan. The atomic point charges were taken from a Mulliken population analysis of the electronic density of the higher-level region.[43]

Single-point energy calculations were then performed on the optimized geometries, increasing the higher-level region to 168 atoms and treating this layer at the density functional theory level, with the BB1K functional[37,39,44] and the larger 6-311+G(2d,2p) basis set. We used this hybrid-meta density functional because it was shown to lead to good agreement in activation and reaction energies for this reaction, when compared to higher-level post-Hartree−Fock methods.[12,45] The level of theory used to obtain the geometry was lower than that used to calculate the energy, and even though this procedure might introduce some inaccuracies in the calculation, it is well-known that the energy is not very sensitive to the quality of the geometry, provided that the geometry has a good accuracy. This approach is implicit when someone calculates the energy with a larger basis set that the one used to optimize the geometry. This procedure has also been used in other enzymatic studies.[40–42]

3. Results and Discussion

It is well-known that β-galactosidase from *E. coli* belongs to the retaining glycosidases class, which catalyzes the hydrolysis of β-D-galactosides with retention of the same stereochemistry as the reactants. In this work, we try to understand the atomistic detail of the mechanism by which this enzyme catalyzes the hydrolysis of the extremely stable glycosidic bond, and to do so, we performed docking simulations, MD simulations, and QM/MM calculations. The mutated enzyme (E537Q), with the crystallographic structure available in the Protein Data Bank (PDB code 1JYN), binds lactose in the shallow mode.[6] To study the catalytic mechanism, we needed to have the substrate closer to the active site, that is, in the deep binding mode. For that purpose, we docked a lactose molecule farther inside the active site of the optimized unligated β-galactosidase (PDB code: 1DP0).[4] As mentioned, the aromatic Trp568 residue close to the active site provides a hydrophobic platform and displays a position and orientation that promote the packing of the galactosyl ring of the lactose in a favorable position for binding. Consequently, a distance constraint (3.40−3.70 Å) was included between this residue and the docked galactose moiety.[24] Furthermore, the crucial hydrogen bridge between the nucleophile and the C_2−OH group of the galactosyl ring was also considered in the docking protocol, with a distance constraint (2.00−2.50 Å) between the two atoms involved.[12] Subsequently, we performed an MD simulation to release the bad contacts in the structure, and in the end, we used the final structure to design a large model that included a radius with 15 Å of protein around the lactose substrate for the subsequent QM/MM calculations, as seen in Figure 1.

3.1. Reactants. Analyzing the reactants' structures, one can see that the galactose moiety stacks with Trp568 and the galactosyl hydroxyl groups make specific contacts with the enzyme and with the water molecules coordinated to the Mg^{2+} ion. The glucose moiety is stacked against the side chain of Trp999. Figure 2 shows that the galactosyl 2′-OH group establishes hydrogen bridges with the Glu537 nucleophilic carboxylate (1.71 Å) and with the Asn460 amine (1.94 Å). One can see also that the 3′-OH group is hydrogen-bonded to one Mg^{2+}-bound water molecule and to the His391 side chain (1.85 Å), the 4′-OH group is H-bound to the Asp201 side-chain carboxylate (1.66 Å), and the 6′-OH group interacts with one water molecule and, intramolecularly, with the 3′-HO group of the glucosyl molecule (2.11 Å). This last glucosyl hydroxyl group is also hydrogen-bonded to the

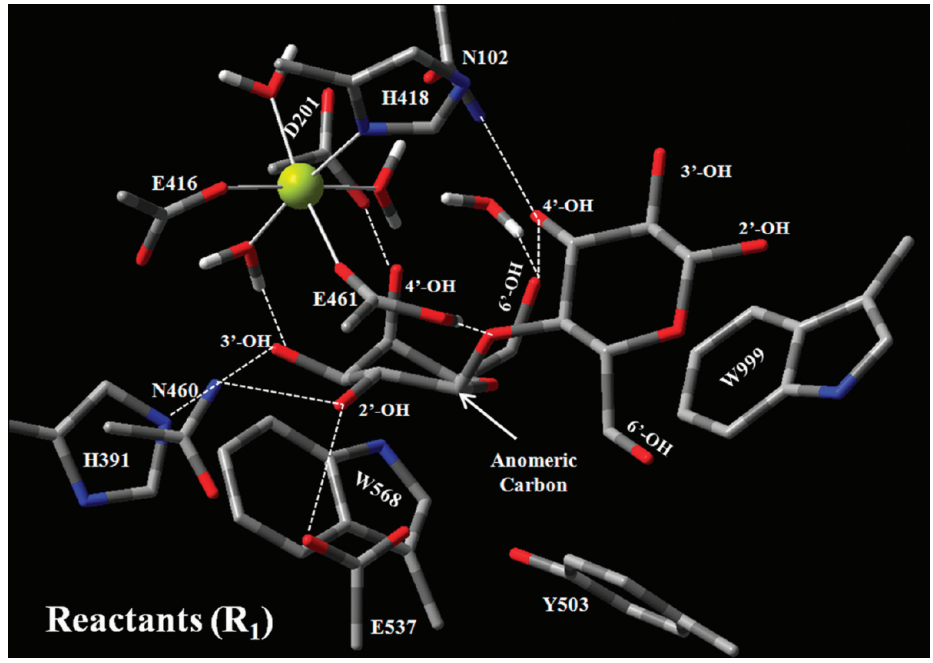

Figure 2. Representation of the optimized structure of the reactants (R_1).

Asn102 amine group (2.15 Å). The glycosidic oxygen establishes a hydrogen bridge (1.67 Å) with the carboxylate group of the catalytic acid/base Glu461, which is protonated. In summary, a complex network of hydrogen interactions with the Asn102, Asp201, His391, Asn460, Glu461, and Glu537 residues determines the binding pose of lactose. These are complemented by hydrophobic interactions between the sugars rings and the side chains of Trp568 and Trp999. This situation is in sharp contrast with the glucosyl moiety, which contains five hydroxyl groups but establishes only one hydrogen interaction with the enzyme residues.

Additionally, the subsite for the glucosyl moiety is significantly larger than the substrate, suggesting that the latter has significant freedom to move. Therefore, one can understand why the second binding subsite is less specific for the bound substrate, which is in agreement with other studies.[6] Experimental data suggest that the glucose subsite is somewhat ill-defined, being specified mostly by a stacking interaction with the aromatic Trp999.[46] These facts are consistent with the behavior of the enzyme, which can bind several aglycon groups.

One can also observe how close the docking/molecular simulations placed the substrate to the magnesium ion. The bivalent ion is hexacoordinated, coordinating to Glu416, His418, Glu461, and three water molecules, with an octahedral geometry. Contrarily, the sodium ion is distant from the substrate, at a distance from the glycosidic oxygen of ca. 8 Å. This ion presents a tetrahedral geometry, coordinated to Asp201, Asn604, and two water molecules. It is worth noticing that all of these water molecules that already existed in the X-ray crystallographic structure were conserved throughout the entire MD simulation.

The antiperiplanar lone-pair hypothesis (ALPH) is a stereoelectronic concept that requires the glycosidic bond to be antiperiplanar in relation to a lone pair of electrons of the oxygen atom of the ring in order to achieve the transition state (TS).[47,48] Furthermore, it is well-known that a conformational change of the glycosidic bond into an equatorial orientation leads to a more planar ring structure, facilitating direct in-line nucleophilic attack.[48] Interestingly, in this β-galactosidase, one can see that a substrate distortion and rotation is necessary to maximize interactions and to fit the active-site pocket. According to the Cremer−Pople polar coordinates[49] that describe sugar conformations, the bound galactosyl ring is almost in a $^4H_3$ conformation. This pretransition state (pre-TS) helps reduce the number of steric clashes between the substrate and the enzyme. Juers et al. proposed that, when the lactose moves from the shallow mode to the deeper mode of binding, an enzyme conformational modification is required, namely, the rotation of the lateral side chain of Phe601.[6] As we started with the lactose molecule bound inside the active site of the enzyme (in the deep mode), no substantial alterations were observed in this lateral side chain, probably because this rotation is only necessary for the movement of the substrate from the shallow to the deeper mode of binding. Subsequently, the side chain should return to the original rotamer.

3.2. First Mechanistic Step. The first step of this catalytic mechanism involves a cleavage of the glycosidic bond of the lactose molecule, as well as the formation of the covalent galactosyl−enzyme intermediate. Given that we used a glucose molecule as the leaving group, acid catalysis is required for this mechanistic step to occur. Various experimental studies on this mechanism have been performed, but the results remain controversial.[6] A possibility, supported by kinetic data, proposes that the reaction is promoted by Lewis catalysis by Mg^{2+}, in which the breakage of the glycosidic bond is facilitated by a direct Mg^{2+} electrophilic attack on the glycosidic oxygen, leading to an Mg−OR complex.[6] On the other hand, the kinetic data are also consistent with Brönsted catalysis, in which the glycosidic bond cleavage is promoted by proton donation to the

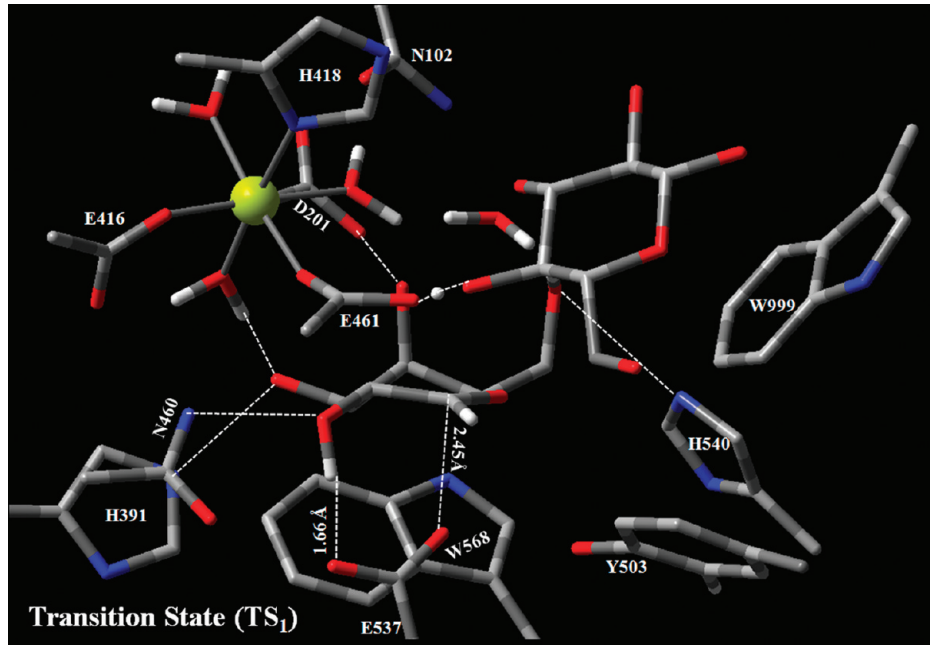

Figure 3. Representation of the optimized structure of the transition state (TS_1).

glycosidic oxygen by Glu461.[10,11] Taking into account the positions of the magnesium ion, Glu461, and the glycosidic oxygen in the crystallographic structures of various ligands bound to the active site of β-galactosidase, catalysis promoted by the proton donor is clearly the most plausible. However, the importance of the Mg^{2+} ion for the enzymatic activity of this galactosidase is well-known. Therefore, its precise function remains unclear.[50,51] In our calculations, we tried to clarify these doubts, as well as understand the role of the magnesium ion in the catalytic mechanism. The reaction coordinate adopted was the glycosidic bond length, that is, the distance between the anomeric carbon and the glycosidic oxygen. Analyzing the transition state for the first mechanistic step (TS_1), which emerges from such a PES, one can see that the breaking of the glycosidic bond occurs with the release of the glucose group. For the reactants, the length of the glycosidic bond is 1.47 Å, increasing to 2.25 Å in TS_1; the bond is almost broken at this stage. Although the proton of the acidic residue comes closer to the glycosidic oxygen, it has not been transferred yet, having a hydrogen-bond distance of 1.46 Å. These results are not identical to the calculations performed with a simple general model for this reaction using the DFT level of calculation, because in that small model, the proton was transferred from the acidic residue to the glycosidic oxygen in the transition state.[12] The difference arises from the greater stabilization of the glycosyl oxygen anion by the enzyme scaffold, which plays a clear catalytic role. Only in the products does the Glu461 residue donate its proton to the glycosidic oxygen, with a distance of 1.03 Å between these two atoms. In the same step, the nucleophilic group comes closer to the anomeric carbon, with one of its oxygens attacking the anomeric carbon. The distance between these two atoms is 3.01 Å in the reactants (R_1), evolving to 2.45 Å in the transition state (TS_1) and to 1.53 Å in the products of this step (P_1), in which a covalent bond is established. Therefore, at the end of this step, a covalent galactosyl−enzyme intermediate is formed. These results confirm the predicted dissociative nature of this transition state, namely, that the glycosidic bond is already broken and the bond to the nucleophilic group is far from established.[7,12]

The transition-state structures developed in the catalytic mechanism are stabilized by both intrinsic electronic effects and binding effects. A great component of catalysis in most glycosidases derives from noncovalent enzyme/substrate interactions that are established along the reaction pathway. Our calculations show that the structure of TS_1 is determined by the specific contacts established between some residues and hydroxyl groups 2, 3, 4, and 6 of the galactose species. The 2′-OH group interacts with the Glu537 nucleophilic carboxylate (1.66 Å) and the Asn460 amine groups (1.87 Å); the 3′-OH interacts with one Mg^{2+} bound water molecule (1.73 Å) and with the His391 side chain (1.87 Å). The 4′-OH group establishes a hydrogen bridge with the Asp201 side-chain carboxylate group (1.62 Å), whereas the 6′-OH group interacts with one water molecule (1.72 Å) and with the His540 side chain (2.92 Å). Some of these hydrogen bridges are very short, supporting their importance in the stabilization of the transition state and explaining the catalytic effect predicted by experimental findings.[7,52] As one can see in Figures 2 and 3, all of these hydrogen interactions are shorter in the transition state than in the reactant structure, revealing their importance to the catalytic mechanism, in the spirit of the archetypal Linus Pauling catalytic concept.

These effects were also studied by comparing the kinetics of the reaction with 2,4-dinitrophenyl β-galactosides in which different OH groups of the substrate were replaced by H or F atoms.[13,53] These studies suggest that absent hydroxyl groups in positions 3, 4, or 6 increase the activation barrier of the galactosylation step by at least 4 kcal/mol. Other studies have revealed that the His391 and His540 residues play important roles in providing a transition-state stabilization through their interactions with the 3′-OH and 6′-OH groups, respectively, of the galactose molecule.[6,18] Some

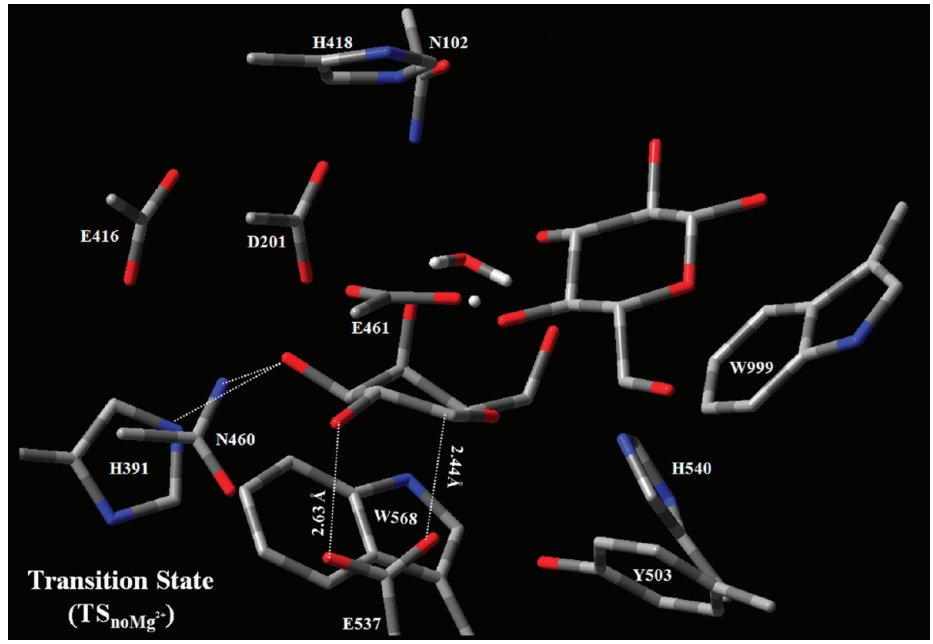

Figure 4. Representation of the optimized structure of the transition state with no Mg^{2+} ($TS_{noMg^{2+}}$).

studies have shown that a histidine residue equivalent to His540 is conserved in every β-galactosidase.[46] These data suggest that the interaction between this residue and the 6′-OH group is very important for the binding of the substrates and for the stabilization of the transition states in both steps of the catalytic mechanism. This study also suggests that this effect is more significant for the degalactosylation step than for the galactosylation step. The most interesting result is that the substitution of the 2′-OH group lowered the reaction rate considerably, contributing approximately 4−5 kcal/mol for TS stabilization. However, this group can reach a maximum of ca. 10 kcal/mol of transition-state stabilization for some β-glycosidases.[7,53] One can see that this hydrogen bridge has a length of 1.71 Å in the reactants, decreasing to 1.66 Å in the TS_1 structure, revealing its importance in the stabilization of this structure, as well as its catalytic effect on the reaction pathway.

A conformational rearrangement of the galactosyl ring is observed in the transition state, resulting in a half-chair conformation (^4E). Many glycosidases show this same conformational distortion in their catalytic mechanisms.[7] However, in our enzymatic model, this reorganization occurs easily because the galactosyl ring in the reactants is already distorted inside the active site. The "electron donation" from the oxygen of the ring to the anomeric carbon results in a partial double bond that facilitates a planar arrangement of the bonds around the anomeric carbon, as one can see in Figure 3. Furthermore, the mentioned hydrogen bridge established between the 2′-HO group and the Glu537 nucleophilic carboxylate group also contributes to this distortion of the galactosyl ring. According to our results, the glycosidic oxygen of the leaving group is equatorial, and hence, this distortion allows for a direct attack of the nucleophilic group to the anomeric center, creating an optimal charge distribution between the ring oxygen and the anomeric carbon for the formation of an oxocarbenium ion. It is obvious that this rearrangement facilitates the progression to TS_1, lowering the activation barrier. Additionally, the hydrogen bond from the proton of the Glu461 carboxylate group to the glycosidic oxygen atom comes closer to the plane of the galactosyl ring; hence, it places the glycosidic oxygen atom in an appropriate position for protonation by the proton donor. Moreover, the two catalytic acids become closer to each other, suggesting an implication for tuning the acid pK_a values through the reaction cycle,[51] as will be discussed shortly. The distortion of the galactosyl ring can also modify the interactions of the other sugars with the residues present in the binding pocket. However, in β-galactosidase, the leaving group is only a glucose molecule, which establishes very few specific interactions because of its nonspecific subsite, and therefore, no substantial modifications occur in its binding pocket.

Analysis of the products of the galactosylation step indicates that a covalent galactosyl−enzyme intermediate forms and that the Glu461 residue donates its proton to the glycosidic oxygen atom, resulting in the departure of the leaving group. When the Glu537 nucleophilic group makes a covalent bond with the galactosyl group, its negative charge is neutralized. As the two carboxylic groups become closer to each other, that modification in charge decreases the pK_a value of the acidic Glu461 residue, inducing proton transfer to the leaving group. This allows the latter residue to act as a base in the degalactosylation step, in a reverse mode of this first step. Some studies have shown that, in enzymes whose activities are highly dependent on existing magnesium ions, the acid catalysis that promotes leaving-group departure is facilitated by their presence.[4,6] It is well-known that β-galactosidase depends catalytically on the presence of the magnesium ion. Additionally, as the Glu461 residue coordinates with the latter, it has been suggested that it could tune the pK_a value of the amino acid.[51] To better understand the key role of the magnesium ion in the reaction pathway,

we repeated the mechanistic step using a similar model, but without the bivalent cation; the results are presented in the next section.

3.3. First Mechanistic Step without the Magnesium Ion. As mentioned, Lewis catalysis promoted by Mg^{2+}, involving a direct electrophilic attack on the glycosidic oxygen by that same ion, does not seems plausible because of the large distance between those two entities in all crystallographic structures. Various studies have suggested that the magnesium ion might have a dynamic role in tuning the pK_a of the Glu461 residue during the reaction. However, this ability remains to be confirmed.[4,6,10,11,50,51] Other studies have suggested that the conformational changes that occurs in the protein structure along the reaction pathway are the cause for the catalytic dependency on the magnesium ion. In this way, these conformational changes would be favored differently depending on the aglycon bound.[6,11]

Analysis of our data indicates a structural reorganization around the Glu461 residue at the transition state without Mg^{2+} ($TS_{noMg^{2+}}$); moreover, some differences in the specific contacts established between the protein and the galactosyl group were observed, as can be seen in Figure 4. The length of the glycosidic bond is 2.40 Å at $TS_{noMg^{2+}}$; comparison with the value obtained for TS_1 (2.25 Å) suggests that this mechanistic step becomes slower in the absence of the magnesium ion. Additionally, the proton of the Glu461 residue comes closer to the glycosidic oxygen atom (1.44 Å), similarly to the behavior observed for the TS_1 structure (1.46 Å). On the other hand, the bond distance between the nucleophilic oxygen and the anomeric carbon is shorter than in TS_1, having a value of 2.32 Å as compared to 2.45 Å at TS_1, also pointing to a later transition state. In summary, a shift toward a delayed transition state was observed upon deletion of the Mg^{2+} ion. Moreover, in the model that includes the magnesium ion, the distance between this ion and the glycosidic oxygen changes from 4.70 to 4.19 Å, suggesting that the crucial role played by this cation is none other than the stabilization of the glycosidic anion in the transition-state structure. It is well-known that this negative charge is directly involved in the increase of the activation barrier values. Furthermore, in the absence of this cation, the acid/base residue (Glu461) becomes less stabilized (it was coordinated to Mg^{2+}), which results in its approach toward the Asn460 residue to establish a hydrogen interaction with its amine side chain (2.24 Å).

Values for the activation barrier and reaction energy were calculated for all optimized geometries with the BB1K hybrid-meta functional and the 6-311+G (2d, 2p) basis set. Various studies have suggested that the BB1K functional is the best for calculation of the activation barrier of this kind of reaction and that it overestimates these values typically by about 1.5 kcal/mol.[12,54] Figure 5 shows the activation barriers and reaction energies for both systems, with and without the magnesium ion. Comparing the activation barrier values obtained for the two reactions, 15.0 and 29.9 kcal/mol, respectively, one can see that the initial value increased significantly in the absence of the cation. Experimental data suggest that the presence of the magnesium ion increases the activity of the β-galactosidase by 5−100-fold, depending

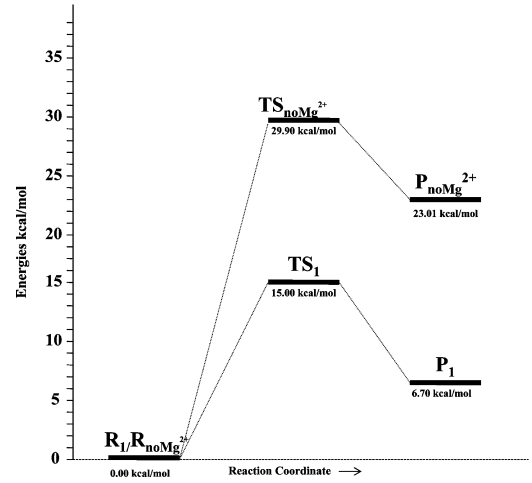

Figure 5. Energetic pathway for the galactosylation mechanistic step of the hydrolysis reaction of the glycosidic linkages with and without magnesium ion.

on the substrate.[16] However, taking into account the calculated activation barrier, one can assume that this mechanistic step is magnesium-dependent and that, in the absence of Mg^{2+}, the reaction either does not occur or occurs through a different pathway. The reproduced barrier difference with and without Mg^{2+} ion is larger than the corresponding experimental value. However, all of the experimental thermodynamic and kinetic data were well reproduced with our model with the exception of the magnitude of the magnesium ion effect. The exaggerated prediction of the effect of the Mg^{2+} ion might occur because the enzyme rearranges more extensively at the TS than was captured with the energy minimizations (or even MD simulations, as these rearrangements have a long time scale).

On the other hand, the reaction energy value obtained for the model with the magnesium ion is 6.7 kcal/mol, compared to 23.0 kcal/mol without the magnesium ion. The variation in the Gibbs energy is positive, which indicates that this first mechanistic step of the net reaction of glycosidic bond hydrolysis is thermodynamically unfavorable. However, it becomes far more unfavorable in the absence of Mg^{2+}, emphasizing the importance of the metal ion to the catalytic cycle.

It is interesting to note that the calculated barrier for the galactosylation step without the magnesium ion is similar to that obtained in the small model with the BB1K functional. However, the Gibbs energy is much higher than that in the small-active-site model. Some interactions might contribute to the destabilization of the products in the enzyme without the Mg^{2+} ion in relation to the small model, for example, an unfavorable contact of Glu416 with Glu461. The unprotonated Glu416 belongs to the coordination shell of Mg^{2+} ion and was retained in the model without the magnesium ion but not included in the small model. As the system moves from the reactants to the products, a negative charge is transferred to Glu416, and the system is strongly destabilized because of the short distance between the two negative glutamate residues (ca. 4.5 Å). This is an important factor, but not the only one that justifies the difference in the reaction energy of the two systems. The sum of a very large number

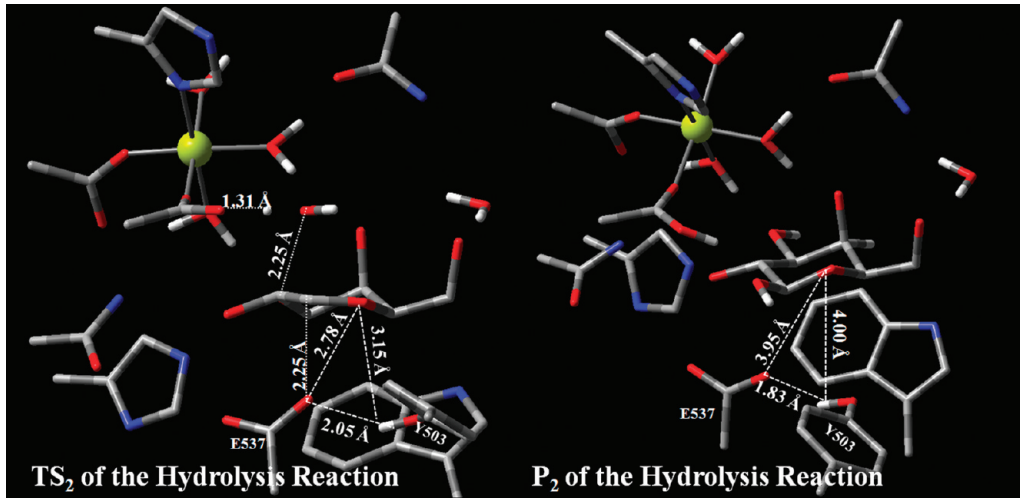

Figure 6. Representation of the structures of the transition state (TS_2) and products (P_2) for the degalactosylation step.

of small interactions present in the larger model might, as a whole, increase the energy of the products, even though their effect is not trivial to pinpoint individually.

3.4. Second Mechanistic Step: Hydrolysis Reaction. The second mechanistic step involves the attack of the covalent galactosyl−enzyme intermediate by a water molecule. To obtain the reactants for this step, we transformed the leaving group into a water molecule, keeping the glycosidic hydroxyl and replacing the remaining one by a proton directed along the C−O bond. In the reactant structures (R_2), the distance between the anomeric carbon atom and the oxygen atom of the attacking water is 3.43 Å. Figure 6 shows the structure of the hydrolytic transition state (TS_2) in which the breaking of the bond between the anomeric center and the nucleophile group occurs. The length of this bond is 1.53 Å in the reactants and 2.25 Å at TS_2. Therefore, the bond might be considered as being broken at this stage. The attacking water molecule comes closer to the anomeric carbon atom, with the oxygen atom performing the attack. However, one can see that the covalent bond has not yet been established (2.25 Å) at this stage. Only in the products (P_2) is the bond fully formed, with a length of 1.41 Å. Additionally, one proton of the water molecule gets closer to the base Glu461 carboxylate group at the TS, with a distance of 1.31 Å. At this stage, proton transfer is ready to occur. The data also confirm the expected dissociative nature of the degalactosylation step, with the bond to the nucleophilic group already broken and the glycosidic bond not yet established.[7,45]

Furthermore, the cleavage of the nucleophilic bond transfers the negative charge back to the Glu537 carboxylate group. During this degalactosylation step, a trigonal oxocarbenium ion has formed, again stabilized by interactions between the Glu537 carboxylic side chain, the Tyr503 hydroxyl side chain, and the oxygen atom of the galactosyl ring. Figure 6 shows the distances among all of these atoms for the TS_2 and P_2 structures. Secondary kinetic isotope effects previously suggested this to be a trigonal oxocarbenium ion.[19,55] The short hydrogen bridge established with the Tyr503 hydroxyl group could facilitate the elimination of the negative nucleophile. Studies performed with a myrosinase (from *Sinapis alba*) and a xylanase (from *Bacillus circulans*) suggest that an equivalent tyrosine residue near the nucleophilic catalytic group plays a similar role in these catalytic mechanisms.[6,56,57]

One can see that, in the products, the galactosyl group adopts the lower-energy chair conformation. At the end of all reactions, the acid/base Glu461 ends up protonated, whereas the Glu537 nucleophilic residue is negatively charged; that is, the two catalytic residues are prepared for another reaction cycle.

Values for the activation barrier and reaction energy for this second step were also calculated, for the optimized geometries, using the BB1K hybrid-meta functional and the 6-311+G (2d, 2p) basis set. The values obtained were 15.5 and −9.2 kcal/mol, respectively. At the end of this step, a glucose molecule dissociates from the active site. The kinetics and the free energy profile for the dissociation step are probably very complex, but they must be included in the free energy profile for the reaction, as their thermodynamic contribution must be far from negligible. To introduce this effect, we used a simplified, but still accurate, model in which we considered only a glucose molecule surrounded by (and geometry-optimized within) two dielectric continuum solvents, one with $\varepsilon = 4$ and the other with $\varepsilon = 80$. A dielectric constant of 4 mimics a hydrophobic protein environment, whereas a value of 80 corresponds to an aqueous environment. The dissociation free energy, ΔG_{diss}(Glu), corresponds to the difference between these two values (−9.09 kcal/mol).

Upon addition of ΔG_{diss}(Glu), the rate-limiting activation barrier (calculated from the initial reactants) and the Gibbs energy of reaction were calculated as 15.00 and −11.53 kcal/mol, respectively (Figure 7). These values indicate that this mechanistic step is both kinetically and thermodynamically favorable. Our results are in agreement with experiment, as the value of k_{cat} for the hydrolysis of lactose has been reported as 60 s^{-1} (corresponding to an activation barrier value of approximately 15 kcal/mol).[16,58,59] Kempton and Withers studied the *Agrobacterium sp.* β-glucosidase using different substrates and described a relationship in which the pK_a values of the leaving groups are good predictors of k_{cat}, as

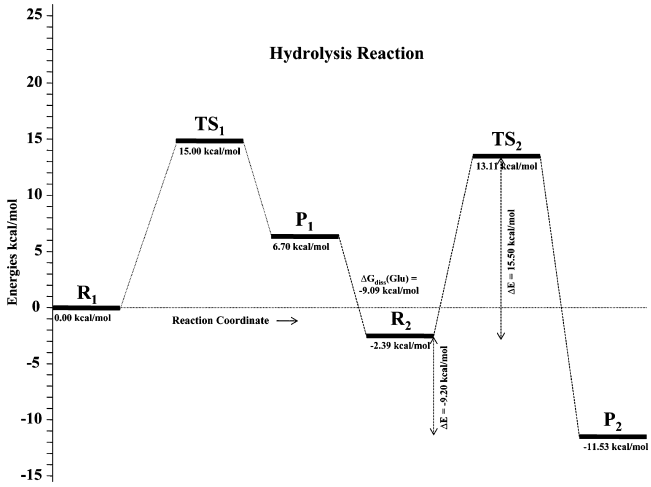

Figure 7. Energetic pathway for the hydrolysis reaction of the glycosidic linkages.

well as the rate-limiting step.[14] They found that the first step should be rate-limiting for leaving groups with pK_a values above 8. It is well-known that lactose is a substrate with a very unfavorable leaving group. The pK_a of the glycosyl oxygen is 11,[60] which indicates that the galactosylation step should be rate-limiting. However, our data indicate similar values of the activation barriers for both steps (galactosylation and degalactosylation). Therefore, although the activation energy for this degalactosylation step is higher than that for the galactosylation step, the small difference between them is smaller than the accuracy of the computational method, and therefore, this computational method is unable to confirm which one is the rate-limiting step.

3.5. Second Mechanistic Step: Transglycosylation Reactions. Transglycosylation reactions occur when the same leaving group, or another carbohydrate molecule, attacks the covalent galactosyl−enzyme intermediate. At the end of the first step, if the glucose molecule does not leave the active site, it can rotate and attack the intermediate with one of its several hydroxyl groups. As we have already mentioned, the glucose molecule makes few specific interactions and has substantial freedom of movement in the binding pocket, which allows for rotations and conformational transitions. On the other hand, this molecule is a poor leaving group, suggesting that transglycosylation reactions are favorable. In the case of β-galactosidase from *E. coli*, some studies have suggested that galactosyl-β(1−6)-glucose (allolactose) is the preferred transglycosylation product, showing a yield of ca. 97% over the other disaccharides.[58] Considering that the allolactose molecule is the natural *lac* operon inducer (thus strictly necessary for the β-galactosidase production), this preference is expected and is physiologically important to the *E. coli* bacterium. To better clarify the origin of the stereoselectivity of this enzyme during the transglycosylation reactions, we performed a study of the PESs for the attacks of the anomeric center on the oxygens of the different hydroxyl groups, namely, those of the C_3, C_4, and C_6 atoms of the glucose group. Figures 8 and 9 show the activation barriers and reaction energies obtained for the β(1−3) and β(1−6) transglycosylation reactions, respectively.

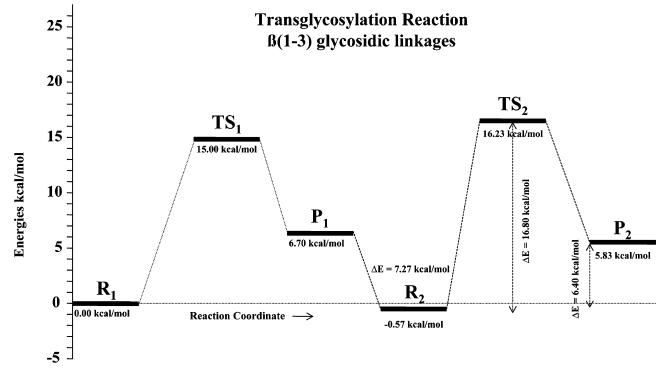

Figure 8. Energetic pathway for the transglycosylation reaction that produces β(1−3) glycosidic linkages.

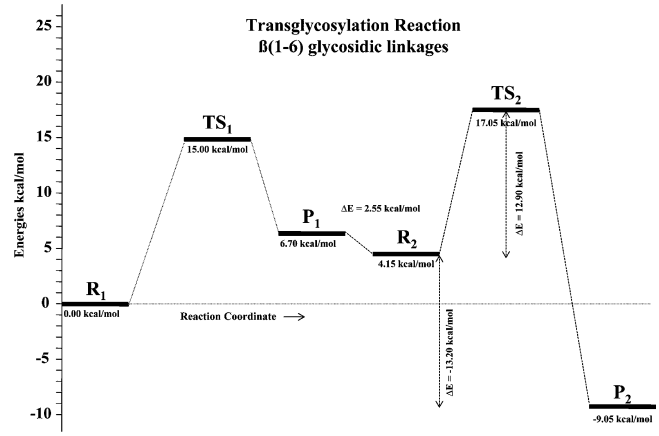

Figure 9. Energetic pathway for the transglycosylation reaction that produces β(1−6) glycosidic linkages.

The first step, in which the covalent galactosyl−enzyme intermediate is formed, is common to all of the reaction pathways because of the necessary cleavage of the natural lactose substrate. In the β(1−4) transglycosylation reaction, the products of the first step are also the reactants of the second step; thus, this transglycosylation pathway is a reverse mode of the galactosylation pathway (Figure SI-2 in the Supporting Information). Therefore, the activation barrier and total Gibbs energy are 15.0 and 0.0 kcal/mol, respectively.

On the other hand, the products of the cleavage step are quite different from the reactants for both β(1−3) and β(1−6) transglycosylation steps. By analyzing the products of the galactosylation step, one can verify that only the O−C_4 bond is directed toward the anomeric carbon atom, whereas the O−C_3 and O−C_6 bonds are pointing in other directions. Therefore, rotation and conformational adjustment in the glucosyl ring are necessary for the attack to be performed by the oxygens of hydroxyl groups 3′-HO and 6′-HO. Figure 10 shows the structures of the reactants for the β(1−3) and β(1−6) transglycosylation steps.

Comparing the energies of the P_1 and R_2 states of these transglycosylation reactions, one can see that these modifications decrease the energies values of R_2 by 7.27 and 2.55 kcal/mol for β(1−3) and β(1−6) glycosidic bonds, respectively, as compared to those of β(1−4) glycosidic linkages. According to these data, one can assume that the reactants' geometries for the β(1−3) transglycosylation pathway are

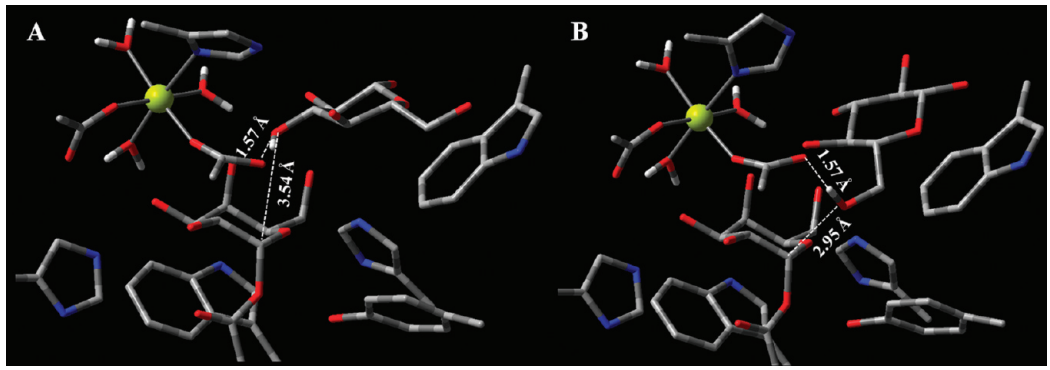

Figure 10. Structures of reactants for different transglycosylation steps: (A) β(1−3) glycosidic linkages, (B) β(1−6) glycosidic linkages.

the most stable, showing the lowest energy values. However, the activation barrier and reaction energies for the β(1−3) transglycosylation reaction are 16.23 and 5.83 kcal/mol, respectively, whereas those for the β(1−6) transglycosylation reaction are 17.05 and −9.05 kcal/mol, respectively. In summary, the activation barriers for the three different pathways studied are 16.23, 15.00, and 17.05 kcal/mol for the β(1−3), β(1−4), and β(1−6) transglycosylation reactions, respectively. one can see that all barriers are similar (which seems logical, as the bonds being broken and formed are of the same type in all three reactions). Additionally, as was already mentioned, the density functional used in our calculations is known to overestimate the activation barriers.[12,54] With a small model, we confirmed that this meta-hybrid density functional overestimates the activation energy of this reaction by 1.7 kcal/mol in relation to high-level post-HF calculations.[45] Subtracting this error from the activation barrier for the β(1−6) transglycosylation reaction, we obtain the value of 15.35 kcal/mol, which is in agreement with the experimental data that proposed a $\Delta G^{\ddagger}$ value of approximately 15 kcal/mol for the allolactose production. These data suggest that the transglycosylation reactions to produce all of the aforementioned kinds of disaccharides are thermodynamically favorable. In summary, the reaction energy values for the three different reactions studied are 5.83, 0.00, and −9.05 kcal/mol for the β(1−3), β(1−4), and β(1−6) transglycosylation reactions, respectively. Concerning these results, one can see that the formation of the β(1−3) glycosidic bond is thermodynamically unfavorable, which suggests that this enzyme does not produce this kind of linkage. In contrast, the fact that the formation of the β(1−6) glycosidic bond has the most negative value of the Gibbs energy shows that this transglycosylation reaction is thermodynamically more favorable than any other, explaining the preference of the β-galactosidase for the production of the allolactose molecule. All of these data are in agreement with the experimental studies that suggested that the galactosyl-β(1−6)-glucose is the preferred transglycosylation product of this enzyme. The basis for the stereoselectivity is therefore thermodynamic, rather than kinetic, and relies on the more favorable binding of the β(1−6) product to the active site. Therefore, the enzyme promotes enrichment in β(1−6) linkages through selective stabilization of the desired product.

4. Conclusions

Despite the large number of studies on the glycosidase family of enzymes and their reactions mechanisms, many atomistic insights are still not fully elucidated. In the theoretical study presented here, BB1K:AMBER QM/MM calculations were performed on a large enzymatic model in order to fully understand the catalytic mechanism of the hydrolysis, its dependence on magnesium, and the origin of the stereoselectivity of the different transglycosylation reactions performed by β-galactosidase from *E. coli*.

Our analysis of the optimized structures of the reactants, transition states, and products for both galactosylation and degalactosylation steps of the mechanism confirms the dissociative nature of the transition states, as is generally accepted for glycosidases. In the first TS, the glycosidic bond is very elongated, and the nucleophilic group is still far from the anomeric carbon atom, as well as the hydrogen atom of the proton donor, which, in turn, is still bound to the acid/base residue. In the second TS, the covalent bond established between the anomeric carbon atom and the nucleophilic group is almost broken, and the attacking oxygen of the water molecule is still far from the anomeric carbon. Additionally, a proton from a water molecule comes close to the acid/base residue, but does not transfer at this stage. Furthermore, our data show the presence of a shorter hydrogen bridge between the nucleophilic group and 2′-HO of the galactosyl group (1.66 Å), as well as the ring planarization toward the half-chair conformation at the transition state. These phenomena have a crucial role in lowering the activation energy of the system and help stabilizing the nascent oxocarbenium ion.

The key role played by the critical magnesium ion in the hydrolysis catalytic mechanism of this enzyme was also studied, and we found that the activation barrier is significantly affected by the absence of this ion. In such a situation, the activation energy rises by 14.9 kcal/mol, emphasizing the necessity of this magnesium ion for the catalytic mechanism to take place. We suggest that this occurs probably through the stabilization of the leaving group by the bivalent cation.

The galactosylation step of the hydrolysis reaction is rate-limiting, having an activation barrier of 15.0 kcal/mol. Moreover, the total reaction energy is −11.5 kcal/mol. Therefore, we conclude that this catalytic reaction is kineti-

cally and thermodynamically favorable, which is in complete agreement with the experimental data on β-galactosidade from *E. coli*. Comparing these values with those obtained with a similar small system, we verified that these values are much more favorable; therefore, the contribution of the enzymatic environment to the reaction kinetics is strictly necessary to characterize quantitatively the catalytic mechanism for this galactosidase. It was concluded that the enzyme scaffold binds the transition state better than the reactants, providing a huge catalytic effect.

Different transglycosylation reactions that produce the $\beta(1-3)$, $\beta(1-4)$, and $\beta(1-6)$ glycosidic linkages were also studied. Comparison of the energetic values for these reactions shows that the transglycosylation reactions are all very similar from a kinetic perspective, which seems reasonable given the similarity in the bond-breaking/bond-forming processes. However, thermodynamically, they are quite dissimilar, with the transglycosylation step to make $\beta(1-6)$ glycosidic bonds being significantly favored. We can conclude that this retaining β-galactosidase has a transglycosylation preference for glycosidic linkages in the order $\beta(1-6) > \beta(1-4) > \beta(1-3)$. Therefore, our data suggest that the allolactose molecule is the preferred product obtained, which is in agreement with the experimental data. According to the free energy values obtained here, the $\beta(1-6)$ product should be selected to $\sim$100%, which is very close to the 97% preference observed experimentally. The origin for the stereoselectivity was found to be thermodynamic, with the enzyme stabilizing the preferred product.

This QM/MM study allows for a complete comprehension of this catalytic mechanism with atomistic detail. As the β-galactosidase from *E. coli* is an enzyme commonly used in molecular biology research, knowledge of the different reaction pathways is crucial to the development of new chromophore substrates. Furthermore, such knowledge helps improve the efficiency of large-scale industrial design and synthesis of new inhibitors and carbohydrates for both the pharmaceutical and food industries.

Acknowledgment. N.F.B. thanks the Fundação para a Ciência e a Tecnologia (FCT) for a Ph.D. grant (SFRH/BD/31359/2006).

Supporting Information Available: Atomic point charges calculated, with a Mulliken population analysis, for all key atoms involved in bond breaking/bond formation during the scan of the reactants, transition states, and products for all reactions studied (Tables SI-I−SI-III); structure of the natural substrate lactose, energetic pathway for the transglycosylation reaction that produces $\beta(1-4)$ glycosidic linkages, and all linear transit schemes for all steps studied (Figures SI-1 and SI-2 and Schemes SI-1−SI-5, respectively). This information is available free of charge via the Internet at http://pubs.acs.org/.

References

(1) Perugino, G.; Trincone, A.; Rossi, M.; Moracci, M. *Trends Biotechnol.* **2004**, *22*, 31.

(2) Maugard, T.; Gaunt, D.; Legoy, M. D.; Besson, T. *Biotechnol. Lett.* **2003**, *25*, 623.

(3) Jakeman, D. L.; Withers, S. G. *Can. J. Chem.* **2002**, *80*, 866.

(4) Juers, D. H.; Jacobson, R. H.; Wigley, D.; Zhang, X. J.; Huber, R. E.; Tronrud, D. E.; Matthews, B. W. *Protein Sci.* **2000**, *9*, 1685.

(5) Jacobson, R. H.; Zhang, X. J.; Dubose, R. F.; Matthews, B. W. *Nature* **1994**, *369*, 761.

(6) Juers, D. H.; Heightman, T. D.; Vasella, A.; McCarter, J. D.; Mackenzie, L.; Withers, S. G.; Matthews, B. W. *Biochemistry* **2001**, *40*, 14781.

(7) Zechel, D. L.; Withers, S. G. *Acc. Chem. Res.* **2000**, *33*, 11.

(8) Koshland, D. E. *Biol. Rev. Cambridge Philos. Soc.* **1953**, *28*, 416.

(9) Crout, D. H. G.; Vic, G. *Curr. Opin. Chem. Biol.* **1998**, *2*, 98.

(10) Richard, J. P.; McCall, D. A. *Bioorg. Chem.* **2000**, *28*, 49.

(11) Sinnott, M. L.; Withers, S. G.; Viratelle, O. M. *Biochem. J.* **1978**, *175*, 539.

(12) Bras, N. F.; Moura-Tamames, S. A.; Fernandes, P. A.; Ramos, M. J. *J. Comput. Chem.* **2008**, *29*, 2565.

(13) Namchuk, M. N.; McCarter, J. D.; Becalski, A.; Andrews, T.; Withers, S. G. *J. Am. Chem. Soc.* **2000**, *122*, 1270.

(14) Kempton, J. B.; Withers, S. G. *Biochemistry* **1992**, *31*, 9961.

(15) Jahn, M.; Withers, S. G. *Biocatal. Biotransform.* **2003**, *21*, 159.

(16) Huber, R. E.; Parfett, C.; Woulfeflanagan, H.; Thompson, D. J. *Biochemistry* **1979**, *18*, 4090.

(17) Cupples, C. G.; Miller, J. H.; Huber, R. E. *J. Biol. Chem.* **1990**, *265*, 5512.

(18) Huber, R. E.; Hlede, I. Y.; Roth, N. J.; McKenzie, K. C.; Ghumman, K. K. *Biochem. Cell Biol.* **2001**, *79*, 183.

(19) Penner, R. M.; Roth, N. J.; Rob, B.; Lay, H.; Huber, R. E. *Biochem. Cell Biol.* **1999**, *77*, 229.

(20) Roth, N. J.; Rob, B.; Huber, R. E. *Biochemistry* **1998**, *37*, 10099.

(21) *Insight II*, version 2.3.0; Accelrys: San Diego, CA, 1993.

(22) Jones, G.; Willett, P.; Glen, R. C.; Leach, A. R.; Taylor, R. *J. Mol. Biol.* **1997**, *267*, 727.

(23) Verdonk, M. L.; Cole, J. C.; Hartshorn, M. J.; Murray, C. W.; Taylor, R. D. *Proteins* **2003**, *52*, 609.

(24) Bras, N. F.; Fernandes, P. A.; Ramos, M. J. *Theor. Chem. Acc.* **2009**, *122*, 283.

(25) Case, D. A.; Darden, T. A.; Cheatham, T. E., III; Simmerling, C. L.; Wang, J.; Duke, R. E.; Luo, R.; Merz, H. M.; Wang, B.; Pearlman, D. A.; Crowley, M.; Brozell, S.; Tsui, V.; Gohlke, H.; Mongan, J.; Hornak, V.; Cui, G.; Beroza, P.; Schafmeister, C.; Caldwell, J. W.; Ross, W. S.; Kollman, P. A. *Amber 8*; University of California: San Francisco, CA, 2004.

(26) Basma, M.; Sundara, S.; Calgan, D.; Vernali, T.; Woods, R. J. *J. Comput. Chem.* **2001**, *22*, 1125.

(27) Kirschner, K. N.; Woods, R. J. *Proc. Natl. Acad. Sci. U.S.A.* **2001**, *98*, 10541.

(28) Kirschner, K. N.; Woods, R. J. *J. Phys. Chem. A* **2001**, *105*, 4150.

(29) Asensio, J. L.; Jimenezbarbero, J. *Biopolymers* **1995**, *35*, 55.

(30) Izaguirre, J. A.; Catarello, D. P.; Wozniak, J. M.; Skeel, R. D. *J. Chem. Phys.* **2001**, *114*, 2090.

(31) Loncharich, R. J.; Brooks, B. R.; Pastor, R. W. *Biopolymers* **1992**, *32*, 523.

(32) Cornell, W. D.; Cieplak, P.; Bayly, C. I.; Gould, I. R.; Merz, K. M.; Ferguson, D. M.; Spellmeyer, D. C.; Fox, T.; Caldwell, J. W.; Kollman, P. A. *J. Am. Chem. Soc.* **1995**, *117*, 5179.

(33) Hammonds, K. D.; Ryckaert, J. P. *Comput. Phys. Commun.* **1991**, *62*, 336.

(34) Frisch, M. J.; Trucks, G. W.; Schlegel, H. B.; Scuseria, G. E.; Robb, M. A.; Cheeseman, J. R.; Montgomery, J. A., Jr.; Vreven, T.; Kudin, K. N.; Burant, J. C.; Millam, J. M.; Iyengar, S. S.; Tomasi, J.; Barone, V.; Mennucci, B.; Cossi, M.; Scalmani, G.; Rega, N.; Petersson, G. A.; Nakatsuji, H.; Hada, M.; Ehara, M.; Toyota, K.; Fukuda, R.; Hasegawa, J.; Ishida, M.; Nakajima, T.; Honda, Y.; Kitao, O.; Nakai, H.; Klene, M.; Li, X.; Knox, J. E.; Hratchian, H. P.; Cross, J. B.; Bakken, V.; Adamo, C.; Jaramillo, J.; Gomperts, R.; Stratmann, R. E.; Yazyev, O.; Austin, A. J.; Cammi, R.; Pomelli, C.; Ochterski, J. W.; Ayala, P. Y.; Morokuma, K.; Voth, G. A.; Salvador, P.; Dannenberg, J. J.; Zakrzewski, V. G.; Dapprich, S.; Daniels, A. D.; Strain, M. C.; Farkas, O.; Malick, D. K.; Rabuck, A. D.; Raghavachari, K.; Foresman, J. B.; Ortiz, J. V.; Cui, Q.; Baboul, A. G.; Clifford, S.; Cioslowski, J.; Stefanov, B. B.; Liu, G.; Liashenko, A.; Piskorz, P.; Komaromi, I.; Martin, R. L.; Fox, D. J.; Keith, T.; Al-Laham, M. A.; Peng, C. Y.; Nanayakkara, A.; Challacombe, M.; Gill, P. M. W.; Johnson, B.; Chen, W.; Wong, M. W.; Gonzalez, C.; Pople, J. A. *Gaussian 03*, revision D.01/D.02; Gaussian, Inc.: Pittsburgh, PA, 2003.

(35) Dapprich, S.; Komaromi, I.; Byun, K. S.; Morokuma, K.; Frisch, M. J. *J. Mol. Struct. (THEOCHEM)* **1999**, *461*, 1.

(36) Maseras, F.; Morokuma, K. *J. Comput. Chem.* **1995**, *16*, 1170.

(37) Becke, A. D. *Phys. Rev. A* **1988**, *38*, 3098.

(38) Becke, A. D. *J. Chem. Phys.* **1996**, *104*, 1040.

(39) Lee, C. T.; Yang, W. T.; Parr, R. G. *Phys. Rev. B* **1988**, *37*, 785.

(40) Lundberg, M.; Blomberg, M. R. A.; Siegbahn, P. E. M. Developing Active Site Models of ODCase—from Large Quantum Models to a QM/MM Approach. In *Orotidine Monophosphate Decarboxylase: A Mechanistic Dialogue*; Topics in Current Chemistry; Springer-Verlag: Berlin, 2004; Vol. 238, pp 79−112.

(41) Mulholland, A. J. *Chem. Cent. J.* **2007**, Vol. 1, Number 19.

(42) Carvalho, A. T. P.; Fernandes, P. A.; Ramos, M. J. *J. Phys. Chem. B* **2006**, *110*, 5758.

(43) Cioslowski, J. *J. Am. Chem. Soc.* **1989**, *111*, 8333.

(44) Zhao, Y.; Lynch, B. J.; Truhlar, D. G. *J. Phys. Chem. A* **2004**, *108*, 2715.

(45) Bras, N. F.; Fernandes, P. A.; Ramos, M. J. *J. Mol. Struct. (THEOCHEM)* 2009; doi:10.1016/j.theochem.2009.08.039.

(46) Roth, N. J.; Huber, R. E. *J. Biol. Chem.* **1996**, *271*, 14296.

(47) Deslongchamps, P. Intramolecular strategies and stereoelectronic effects − Glycosides hydrolysis revisited. *Pure and Applied Chemistry*, 1993; Vol. 65, pp 1161−1178.

(48) Fushinobu, S.; Mertz, B.; Hill, A. D.; Hidaka, M.; Kitaoka, M.; Reilly, P. J. *Carbohydr. Res.* **2008**, *343*, 1023.

(49) Cremer, D.; Pople, J. A. *J. Am. Chem. Soc.* **1975**, *97*, 1354.

(50) Loeffler, R. S. T.; Sinnott, M. L.; Sykes, B. D.; Withers, S. G. *Biochem. J.* **1979**, *177*, 145.

(51) Richard, J. P.; Huber, R. E.; Lin, S.; Heo, C.; Amyes, T. L. *Biochemistry* **1996**, *35*, 12377.

(52) McCarter, J. D.; Adam, M. J.; Withers, S. G. *Biochem. J.* **1992**, *286*, 721.

(53) Namchuk, M. N.; Withers, S. G. *Biochemistry* **1995**, *34*, 16194.

(54) Sousa, S. F.; Fernandes, P. A.; Ramos, M. J. *J. Phys. Chem. A* **2007**, *111*, 10439.

(55) Sinnott, M. L. *FEBS Lett.* **1978**, *94*, 1.

(56) Burmeister, W. P.; Cottaz, S.; Driguez, H.; Iori, R.; Palmieri, S.; Henrissat, B. *Structure* **1997**, *5*, 663.

(57) Sidhu, G.; Withers, S. G.; Nguyen, N. T.; McIntosh, L. P.; Ziser, L.; Brayer, G. D. *Biochemistry* **1999**, *38*, 5346.

(58) Huber, R. E.; Kurz, G.; Wallenfels, K. *Biochemistry* **1976**, *15*, 1994.

(59) Huber, R. E.; Gaunt, M. T.; Sept, R. L.; Babiak, M. J. *Can. J. Biochem. Cell Biol.* **1983**, *61*, 198.

(60) Ye, J. N.; Zhao, X. W.; Sun, Q. X.; Fang, Y. Z. *Mikrochim. Acta* **1998**, *128*, 119.

CT900530F